



Product distribution and the reaction kinetics at the anode of direct ethanol fuel cell with Pt/C, PtRu/C and PtRuRh/C

Nobuyoshi Nakagawa*, Yuki Kaneda, Masatsugu Wagatsuma, Takuya Tsujiguchi

Department of Chemical and Environmental Engineering, Graduate School of Engineering, Gunma University, 1-5-1 Tenjin-cho, Kiryu, Gunma 376-8515, Japan

ARTICLE INFO

Article history:

Received 6 July 2011

Received in revised form 27 August 2011

Accepted 17 October 2011

Available online 20 October 2011

Keywords:

Direct ethanol fuel cell (DEFC)

PtRuRh/C anode catalyst

Electro-oxidation mechanism

Reaction products

Catalytic activity

ABSTRACT

Product distribution at the anode of the direct ethanol fuel cell (DEFC) with different catalysts, i.e., Pt/C, PtRu/C and PtRuRh/C, at 353 K was investigated, and the effect of Rh addition to the PtRu and Ru addition to the Pt on the anode reaction were discussed based on a simple two-step reaction model. It was confirmed that the DEFC with the PtRuRh(2:1:1)/C catalyst showed the highest power density in the DEFCs with the prepared catalysts including Pt/C, PtRu(1:1)/C, PtRuRh(2:1:1)/C and PtRuRh(1:1:2)/C. The Ru and Rh additions increased the current density of the DEFC; however, they reduced the selectivity for CO₂. Based on the calculated rate constants, it was revealed that the Ru addition increased both the rates of ethanol to acetaldehyde and acetaldehyde to acetic acid, and these rates were further increased by the Rh addition. On the other hand, Ru and Rh additions decreased the rate constant of acetaldehyde to CO₂.

© 2011 Elsevier B.V. All rights reserved.

1. Introduction

Direct ethanol fuel cells (DEFCs) have been receiving much attention as an alternative compact power source because of the attractive properties of ethanol, i.e., its high energy density that significantly exceeds that of conventional secondary batteries, its non-toxicity, and its many production routes including a biological method from carbon-neutral and renewable biomass. However, the power output and also the energy conversion efficiency of the current DEFCs are still low in practical use mainly due to the large overvoltage for the electro-oxidation of ethanol at the anode. Hence, many studies to develop an active anode catalyst for ethanol electro-oxidation have been carried out focusing on Pt and Pt-based catalysts [1–12] as well as modifying the catalyst support [13–15].

Some Pt-based binary alloys, such as PtRu [1,2,4,5] and PtSn [1,3–5], showed higher current densities in the ethanol electro-oxidation compared to that of Pt. The current density was further increased by adding third metals to form PtRuSn [4,6,7], PtRuRh [8], PtRuNi [4], PtSnNi [9], PtSnMo [10], PtSnIr [11], PtSnRh [12]. The addition of the second elements, Ru and Sn, and the third elements, Rh, Ni, Mo and Ir, could increase the current density and could lead to an increase in the power density of the DEFC.

On the other hand, the complete electro-oxidation of ethanol, i.e., ethanol to CO₂, does not easily occur at or near ambient temperatures. This is due to the C–C bond of ethanol, and hence,

the major products are usually CH₃CHO and CH₃COOH with a small amount of CO₂ (a few % or less) [1,4,5]. Rousseau et al. investigated the DEFC performance with Pt/C, PtSn/C and PtSnRu/C anode catalysts and obtained the highest power density from PtSnRu/C showing that the addition of Sn and Ru to Pt significantly increased the power density. However, these additions did not lead to an increase in the selectivity for CO₂ [2]. Other studies using differential electrochemical mass spectroscopy (DEMS) revealed that Pt alloy with Ru or Sn showed a higher activity than Pt but also did not lead to a better selectivity for CO₂ [1,4]. In DEFC applications, not only a high power density, but also a high selectivity to CO₂ are important from the viewpoints of energy density and energy conversion efficiency.

Compared to Pt, Rh has a quite low activity for ethanol oxidation, but it showed a higher selectivity for C₂ compounds to CO₂ [16]. Souza et al. reported an improved CO₂ yield on PtRh relative to that on Pt at a similar current using DEMS and in situ FTIR techniques, and they suggested that PtRh is a promising candidate for ethanol oxidation if a third element is added to improve the overall reaction rate [17]. However, it was not until our previous study for PtRuRh/C [8] that ethanol oxidation activity of PtRuRh was evaluated and investigated. In the previous study [8], a higher ethanol oxidation activity of PtRuRh(2:1:1 at. ratio)/C than that of PtRu(1:1)/C was demonstrated by cyclic voltammetry and also a DEFC performance. However, CO₂ selectivity for the PtRuRh/C and the effect of the Rh addition to PtRu/C on the yield and/or selectivity for CO₂ have not been revealed yet. It is necessary to investigate the effect of Rh addition to PtRu/C on the product distribution and CO₂ selectivity.

* Corresponding author. Tel.: +81 277 30 1458; fax: +81 277 30 1457.

E-mail addresses: nakagawa@cee.gunma-u.ac.jp, nobnaka@sannet.ne.jp (N. Nakagawa).

In this study, the electrode performance of PtRuRh/C anode and the reaction products in DEFC were evaluated and compared with that from DEFCs with PtRu/C and Pt/C anodes. The effects of Rh addition to PtRu and Ru addition to Pt on the product distribution and the electro-oxidation mechanism were discussed based on the rate constants calculated for each reaction path in the ethanol oxidation on the catalyst.

2. Experimental

2.1. Catalyst preparation

Carbon-supported PtRuRh nano particles, PtRuRh/C, were prepared by an impregnation method using the nitrates of these metals. Specific amounts of the nitrates, i.e., $\text{Pt}(\text{NO}_3)_2$, $\text{Ru}(\text{NO})(\text{NO}_3)_3$ and $\text{Rh}(\text{NO}_3)_3 \cdot 2\text{H}_2\text{O}$ for Pt, Ru and Rh, respectively, were dissolved in 20 wt% aqueous ethanol solutions, and then Ketjen black as the support carbon was added to the solution; then the mixture was stirred in an ultrasonic bath for 30 min. The slurry was then dried in an oven at 380 K to remove the water and ethanol from the mixture. The dried mixture was then exposed to $\text{H}_2(15\%)\text{-N}_2$ gas at 490 K for 30 min in order to obtain the reduced metals. By adjusting the mass ratio among the nitrates in the solution and that between the metals and Ketjen black in the mixture, different compositions of the PtRuRh supported catalysts, i.e., PtRuRh(2:1:1)/C, PtRuRh(1:1:2)/C, PtRu(1:1)/C and Pt/C, where the ratio in parenthesis (a:b:c) denotes the atomic ratio of a:b:c for Pt:Ru:Rh, respectively, were prepared.

The prepared catalysts were characterized by EDX and XRD (Rint2100, Rigaku).

2.2. MEA preparation and fuel cell operation

The DEFC performance was evaluated for the membrane electrode assembly (MEA) with the different anode catalysts. A certain amount of the catalyst, in the form of a slurry with 2-propanol and water, was painted on the carbon paper (TGP-H-090, Toray). This was then used as the anode after drying. The electrolyte membrane, NR212 (Du Pont), was sandwiched between the anode and a commercially available $\text{Pt}(1.0 \text{ mg cm}^{-2})/\text{C}$ electrode (EC-20-10, ElectroChem, Inc.) as the cathode by hot pressing them at 410 K, 5 MPa, for 3 min to form the MEA. The loading of the metal catalyst for the anode of the MEA with PtRuRh(2:1:1)/C, PtRuRh(1:1:2)/C, PtRu(1:1)/C and Pt/C was 2.6, 3.0, 3.2 and 2.7 mg cm^{-2} , respectively.

The MEA was fixed in the cell holder with serpentine flow channels in both the anode and cathode (FC05-01SP, Electro Chem, Inc.). It was operated as a DEFC by pumping a 0.5 M aqueous ethanol solution at 1.5 ml min^{-1} to the anode and dry oxygen gas at 100 ml min^{-1} to the cathode at 353 K. In some experiments, the cell was operated with 0.3 M acetaldehyde and with 0.01 M acetic acid, 1.5 ml min^{-1} , instead of the ethanol solution, and the results were used for the comparison with that of ethanol.

The electrochemical measurements were conducted using an electrochemical measurement system (HAG-5010, Hokuto Denko, Co., Ltd.).

2.3. Analysis of the reaction products

By feeding the fuel and oxygen to the fuel cell, power generation was conducted at a constant cell voltage for a few hours. After the current density became almost constant, the emission from the anode outlet was collected in a bag for 2 h. The 2 h collection was conducted not only under the closed circuit conditions, but also under the open circuit conditions as mentioned later.

The emission from the anode outlet was liquid without gas bubbles in this experiment. Therefore, in order to evaluate the reaction

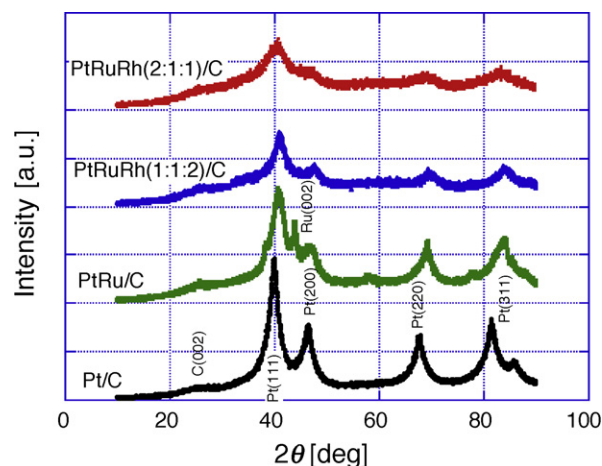


Fig. 1. X-ray diffraction profiles for the catalysts prepared in this experiment.

products, the organic compound dissolved in the fuel solution and the collected solution in the bag were analyzed by gas chromatography using columns of PEG6000 and an FID detector. Also, the dissolved CO_2 in the solutions was measured with a CO_2 electrode (CE-2041, DKK-TOA Corp.).

3. Results and discussion

3.1. Characteristics of the catalyst

The metal composition and loading as well as the particle size of the prepared catalyst were analyzed by EDX and XRD and summarized in Table 1. The metal compositions of PtRuRh(2:1:1)/C, PtRuRh(1:1:2)/C and PtRu(1:1)/C, were approximately similar to that denoted in parenthesis. The metal loading on the carbon support was around 65 wt% and was similar in each case.

Fig. 1 shows the XRD patterns of the prepared catalyst powders. The structure of PtRu was considered to be a mixture of PtRu alloy particles and Ru particles, because the diffraction peak for its Pt(111), which appeared at $2\theta = 39.9^\circ$ for Pt/C, shifted to a higher angle, 40.9° , showing another peak for Ru(002) at $2\theta = 43.8^\circ$ in the XRD profile. Whereas, the structures of the ternary systems that showed the aforementioned shift to 41.8° for PtRuRh(1:1:2)/C and to 40.9° , for PtRuRh(2:1:1)/C were suggested to be alloys. The metal particle size calculated for the peak at 40° based on Scherrer's equation is summarized in Table 1.

3.2. Power generation and reaction products with ethanol fuel

Fig. 2 shows the current–voltage curves for the DEFCs with the different anode catalyst at 353 K, 0.5 M ethanol. The DEFC with the binary and the ternary anode catalyst showed a higher OCV and a higher power density than those with the Pt catalyst. The DEFC with PtRuRh(2:1:1)/C showed the highest cell voltage at a certain current density among the DEFCs with different catalysts in accordance with the previous report [8]. However, one may notice that the increment in the cell voltage from that with PtRu/C to that with PtRuRh(2:1:1)/C was not as significant when the results were compared to that of the previous report [8] using similar catalysts. This is due to the different ethanol concentration used in each experiment.

Fig. 3 shows the current densities for the DEFC with the different anode catalysts measured at 0.125 V, 0.5 M ethanol. The current density decreased with time, especially at the beginning and then became stable after a certain time. The stable current was high in the order of the DEFC with PtRuRh(2:1:1)/C, PtRu/C,

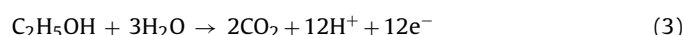
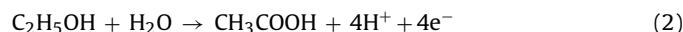
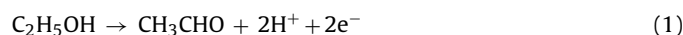
Table 1
Composition of the metal loading of the catalyst analyzed by EDX and the catalyst particle size calculated from the XRD.

Catalyst	Metal composition [atomic ratio]			Metal loading [wt%]	Particle size [nm]
	Pt	Ru	Rh		
PtRuRh(2:1:1)/C	2.00	1.42	1.38	61.5	2.61
PtRuRh(1:1:2)/C	0.81	1.32	2.00	65.4	3.58
PtRu(1:1)/C	1.00	1.30	–	68.8	5.24
Pt/C	1.00	–	–	62.5	4.25

PtRuRh(1:1:2)/C and Pt/C. The period of emission collection at the anode was in the range between the two vertical lines in the figure. The current density during the collection was almost stable in all cases. The electrical charge transferred from the anode to the cathode in the period of the emission collection at different cell voltages is summarized in Fig. 4. The amount of the electrical charge was compared to the amount calculated from the reaction products at the anode.

The reaction products detected in the collected solution were acetaldehyde, acetic acid and carbon dioxide in accordance with that previously reported [1,2,5,16]. Based on the amounts of the reaction products for the 2 h operation, the electrical charge

transferred via the electrode reaction producing the products can be calculated by assuming 2, 4 and 12 electron reactions for acetaldehyde, acetic acid and carbon dioxide, respectively.



The electrical charge calculated from the current exceeded 30% or more compared to the charge calculated from the amounts of the products. This was attributed to the crossover of the products from the anode to the cathode through the membrane [18]. Because the relatively thin membrane, NR212, which was 50 μm in thickness under dry condition, was used in this experiment, a large crossover occurred resulting in such a conflict in the amount of charge.

Furthermore, those reaction products were detected not only under closed circuit conditions, but also the open circuit conditions. Under the open circuit conditions, a such product would be formed by the ethanol oxidation with oxygen transported from the cathode [19], and/or a part of the products at the cathode by the oxidation of ethanol that permeated from the anode to the cathode would cross to the anode through the membrane [20]. In order to separate such products caused by the permeation from cathode to anode and not by the electrochemical oxidation, the production rate of the acetaldehyde, acetic acid and CO_2 measured under open circuit was subtracted from that obtained under closed circuit for a certain condition.

To avoid the unbalance in the charge amounts mentioned above, both the production rate of the reaction product at the anode and chemical selectivity, CS, that defined below were used in the

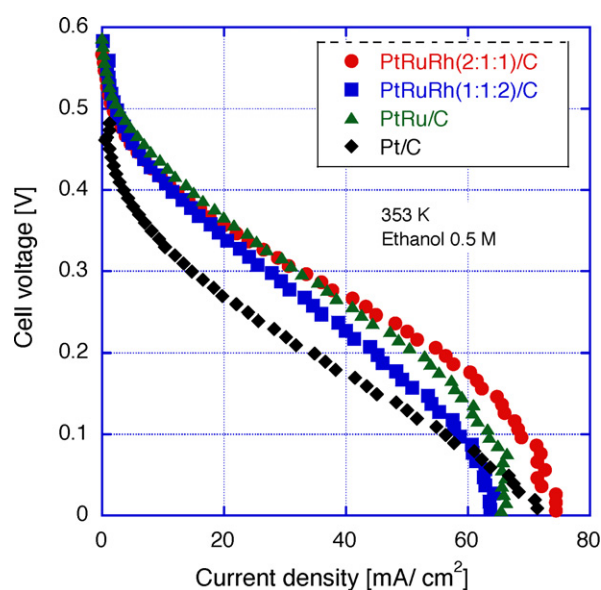


Fig. 2. Current voltage curves of the DEFCs with the different anode catalysts measured at 353 K, 0.5 M ethanol.

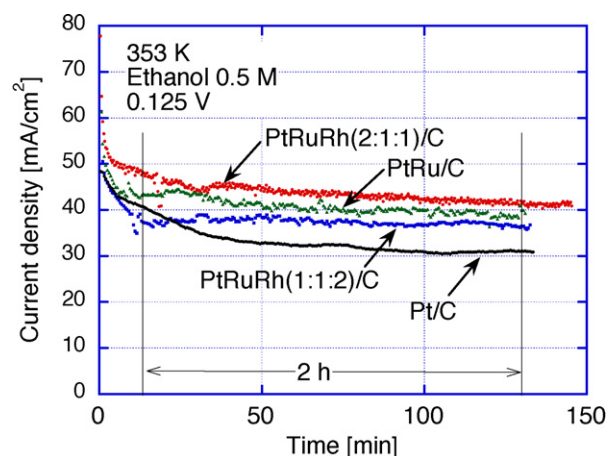


Fig. 3. Current density with time for the DEFCs with the different anode catalyst measured at 353 K, 0.125 V with 0.5 M ethanol.

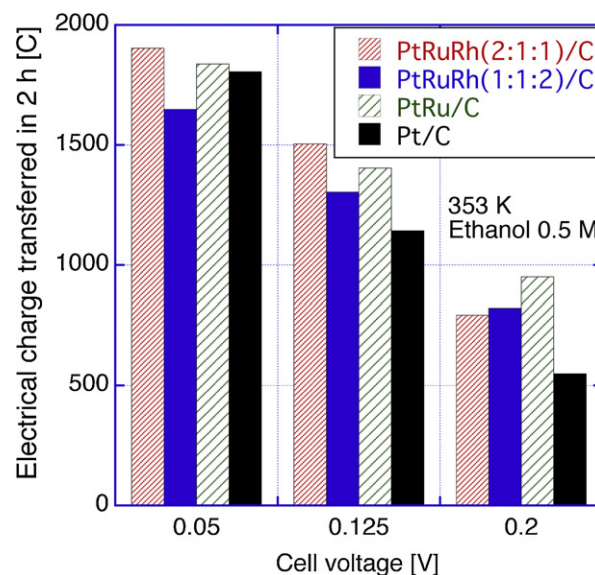


Fig. 4. Electrical charge transferred in the 2 h operation measured for the DMFCs with different catalysts from the integration of the current at 353 K, 0.5 M ethanol and different cell voltages.

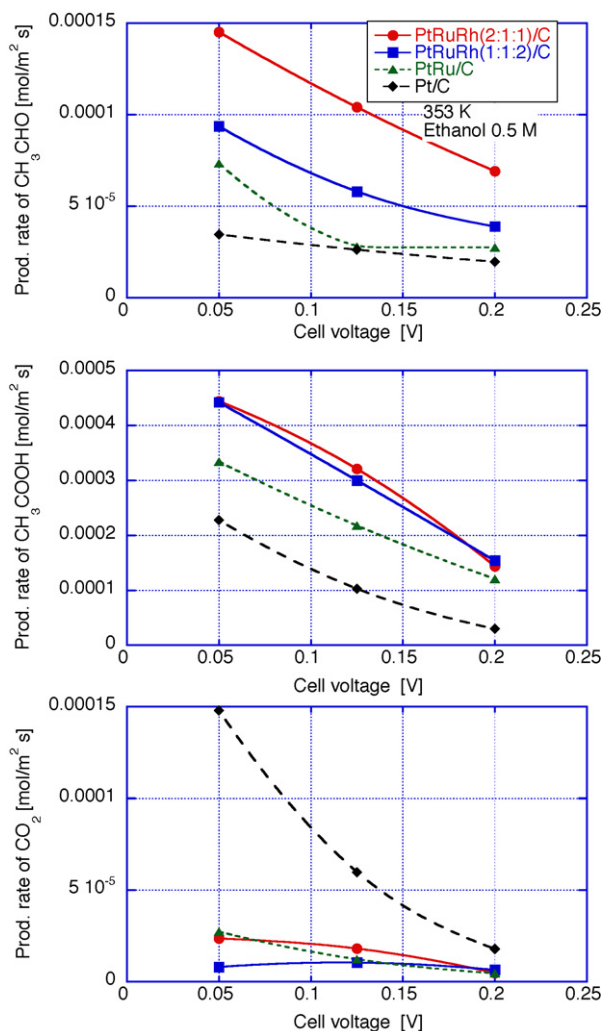


Fig. 5. Production rate of each product at the anode of the DEFCs with the different catalysts measured at 353 K, 0.5 M ethanol and different cell voltages.

reaction analysis. The chemical selectivity was based on the total amount of the reaction products at the anode and was calculated by Eq. (4).

$$CS_i [\%] = \frac{nM_i}{M_{\text{CH}_3\text{COOH}} + M_{\text{CH}_3\text{CHO}} + 2M_{\text{CO}_2}} \times 100 \quad (4)$$

where M is the amount of the product i ; CH₃COOH, CH₃CHO and CO₂, and n is the coefficient which is 2 for CO₂ and 1 for others.

Fig. 5 shows the production rates of acetaldehyde, acetic acid and carbon dioxide at the anode of the DEFC with different anode catalysts at 353 K, 0.5 M ethanol and the different cell voltages, 0.05, 0.125, and 0.2 V. The production rates and current density decreased with increasing cell voltage. When the production rates for the PtRu/C catalyst were compared to that for PtRuRh(1:1:2)/C, one can notice that the production rate for the former was smaller than that for the latter in contrast to the results of the electric charge shown in Fig. 4. The discrepancy was attributed to a relatively large collection loss of the products in the case of the DMFC with the PtRu/C catalyst compared to the cases with the other catalysts. The loss of the former case was about 7% higher than that of the latter due to the unknown reason.

Among the three components of the products, the production rate of acetic acid was the highest, followed by that of acetaldehyde and finally that of CO₂ for the cases with the PtRu/C, PtRuRh(2:1:1)/C and PtRuRh(1:1:2). For these catalysts, one can

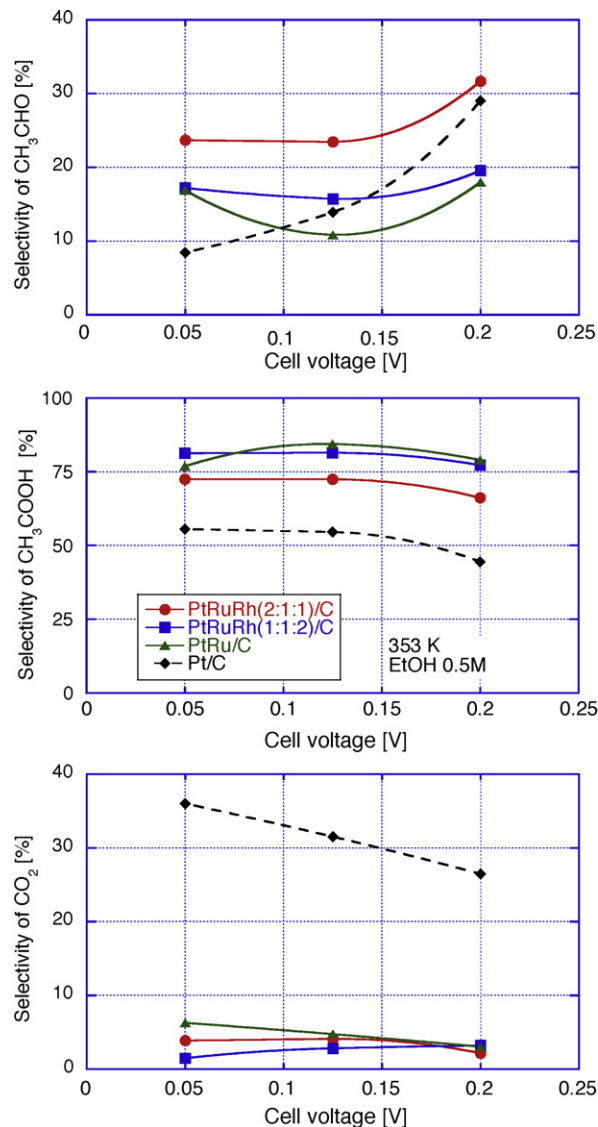


Fig. 6. Selectivity of each product at the anode of the DEFCs with the different catalysts measured at 353 K, 0.5 M ethanol and different cell voltages.

notice that the Rh addition to PtRu increased the production rates of both CH₃COOH and CH₃CHO compared to the case for PtRu. However, the rate of CO₂ production was not affected by the Rh addition. The Pt/C showed the lowest production rates of CH₃COOH and CH₃CHO while the highest production rate of CO₂ especially at the lower cell voltages, 0.05 V and 0.125 V. The higher CO₂ production rate at the lower cell voltages for the Pt/C agreed with the results of a DEMS study by Rao et al. [5]. They showed that CO₂ current efficiency increased with increasing electrode potential in the range below 0.6 V RHE.

Fig. 6 shows the selectivity of each product calculated for the experiments shown in Fig. 5. For the binary and the ternary metal catalysts, the selectivity for CH₃COOH was the highest showing about 75% and that for CO₂ was about a few % irrespective of the cell voltage. On the other hand, in the case of the Pt/C catalyst, the selectivity for CO₂ was higher than 25% showing that Pt itself has a high ability to oxidize ethanol into CO₂. The CO₂ selectivity of the Pt/C decreased with increasing cell voltage while the CH₃CHO selectivity was increased with increasing cell voltage.

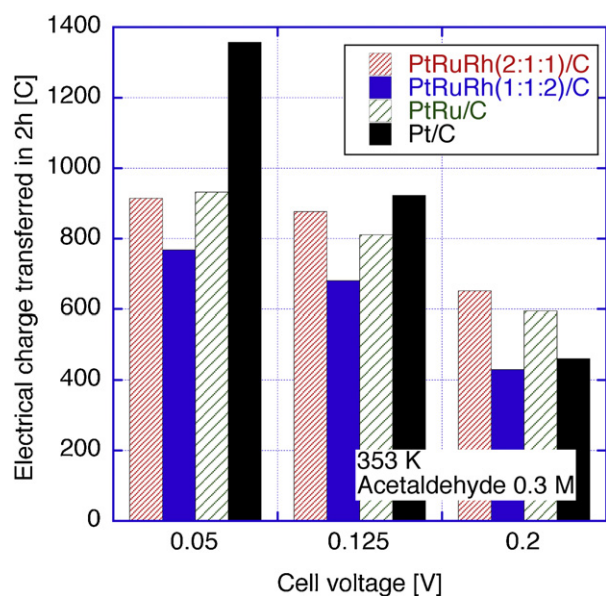


Fig. 7. Electrical charge transferred in the 2 h operation for the fuel cells with the different anode catalysts at 353 K, 0.3 M acetaldehyde and different cell voltages.

3.3. Power generation and reaction products with acetaldehyde fuel

In order to discuss the electro-oxidation mechanism of ethanol, experiments with acetaldehyde and acetic acid, the intermediate products of the ethanol oxidation, as fuel were conducted.

Fig. 7 shows the electrical charge transferred in a 2 h operation of the fuel cell with 0.3 M CH_3CHO . The amount of the electrical charge was about a half that for 0.5 M ethanol shown in Fig. 7. One can see that a relatively large amount of electrical charge was transferred for the Pt/C especially at 0.05 and 0.125 V. Similar amounts of the

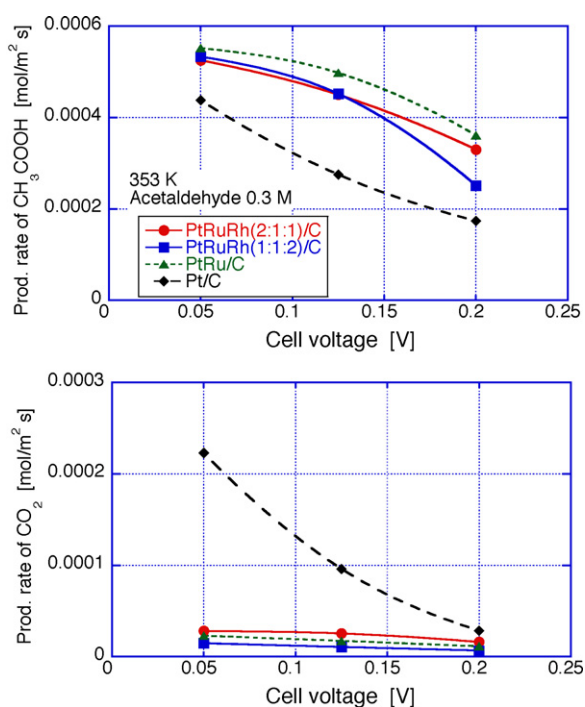


Fig. 8. Production rate of each product, acetic acid and CO_2 , at the anode of the fuel cells with the different catalysts measured at 353 K, 0.3 M acetaldehyde and different cell voltages.

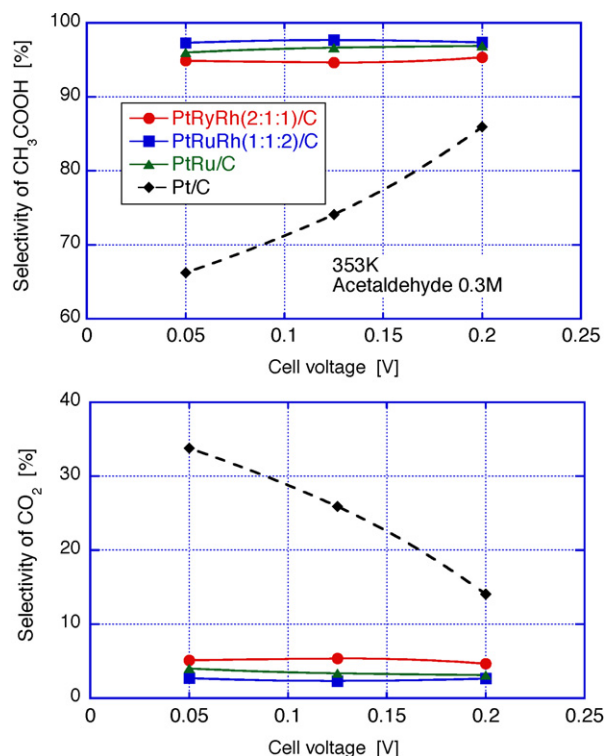


Fig. 9. Selectivity for each product, acetic acid and CO_2 , at the anode of the fuel cell with the different catalysts measured at 353 K, 0.3 M acetaldehyde and different cell voltages.

electrical charge at 0.05 V compared to that at 0.125 V for PtRu/C, PtRuRh(1:1:2)/C and PtRuRh(1:1:2)/C were due to the limiting current which appeared at around 0.1 V for these cases. In these three cases, the active sites for the oxidation would be distracted by the CH_3COOH that was more preferentially produced on these catalysts. It is known that acetic acid is a poisoning compound for the Pt based catalyst [5].

Figs. 8 and 9 show the production rates of CH_3COOH and CO_2 , which were the reaction products, and their selectivity, respectively. The production rates of CH_3COOH decreased with increasing cell voltage for all the catalysts. The production rates of CO_2 were quite small irrespective of the cell voltages for the different catalysts except that for Pt/C. These trends were similar to that obtained from 0.5 M ethanol shown in Fig. 5, although there were small differences among the catalysts. Similarly, the selectivity for CH_3COOH and CO_2 of the different catalysts shown in Fig. 9 was similar to that shown in Fig. 6 except for the selectivity for CH_3COOH of Pt/C, which increased with increasing cell voltage. Similar trends in the production rates and selectivity of the different catalyst between 0.5 M ethanol and 0.3 M acetaldehyde suggested that the oxidation of ethanol occurred stepwise from ethanol to acetaldehyde and then CH_3COOH and CO_2 .

Although 0.05 M acetic acid was used as fuel, the fuel cell did not generate power at all for all the catalysts and showed only very small cell voltages of less than 0.05 V. This means that the oxidation of acetic acid hardly occurs at the catalyst under this condition [5].

3.4. Effect of Ru and Rh addition to Pt on the oxidation mechanism of ethanol

In order to discuss the effect of Ru and Rh addition to Pt and PtRu, respectively, on the catalytic activity for ethanol oxidation, the simple oxidation mechanism shown in Fig. 10 was taken into consideration. A two-step oxidation with the three-pathway scheme

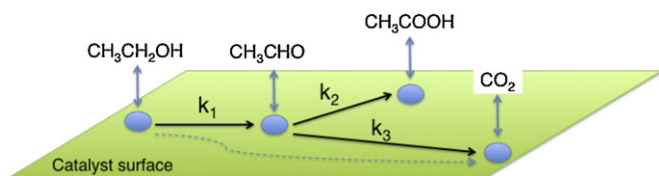


Fig. 10. Assumed reaction scheme of the ethanol oxidation on the catalysts.

was assumed for the electro-oxidation of ethanol. This was similar to that proposed in the previous paper [5] with the exception of the direct pathway to CO_2 . In the first step, ethanol was oxidized to acetaldehyde and then further oxidized to acetic acid or carbon dioxide in the second step. Each reaction step takes place via adsorbed intermediates on the catalyst surface, and the concentration of each of the adsorbed intermediates was assumed to be in equilibrium with the product in the bulk solution. Although the direct pathway from ethanol to CO_2 with the dissociative adsorption of ethanol was considered in the previous reports [5,21,22], the direct pathway was neglected in this study. This is because the ratio of the CO_2 selectivity to the CH_3COOH selectivity for the ethanol fuel calculated from Fig. 6 was similar to the ratio of CO_2 selectivity to the CH_3COOH selectivity for the acetaldehyde fuel calculated from Fig. 9 for the different catalysts. The direct pathway through the dissociative adsorption of ethanol to CO_2 would not be major under the experimental conditions in this study. Also the pathway

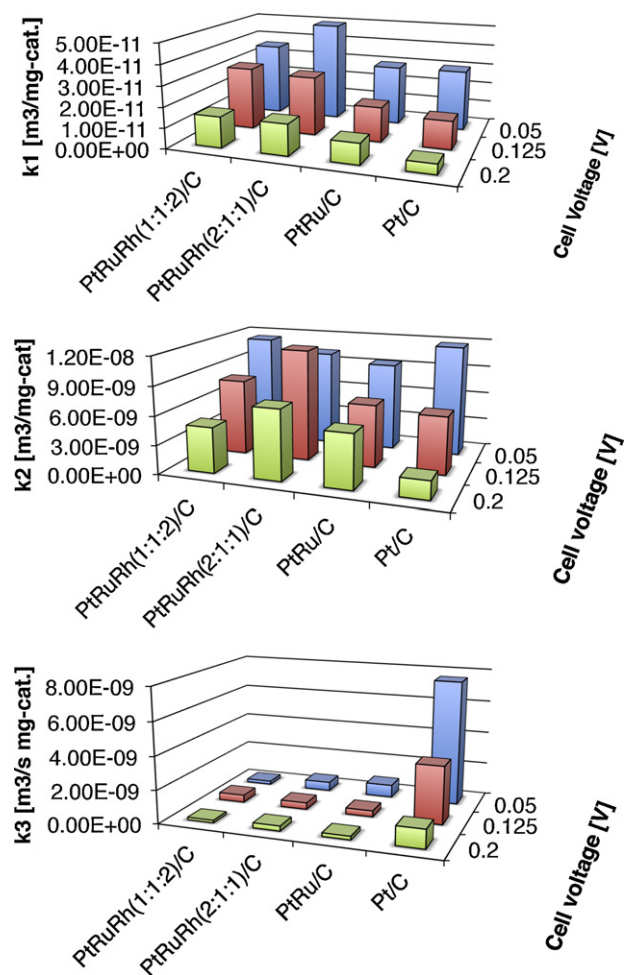


Fig. 11. Calculated reaction rate constants, k_1 , k_2 and k_3 , for each reaction step shown in Fig. 10 for the different catalysts.

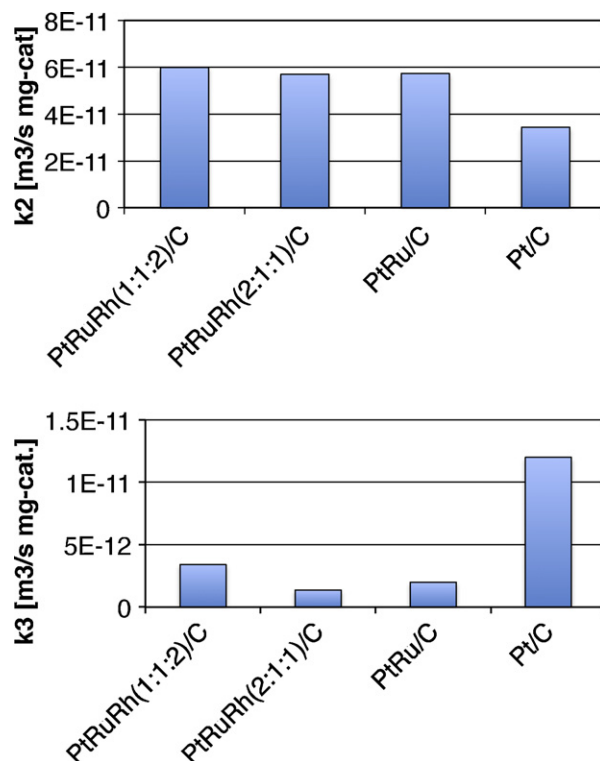


Fig. 12. Calculated reaction rate constants, k_2 and k_3 , at 0.125 V for the different catalysts obtained from the 0.3 M acetaldehyde oxidation.

from acetic acid to CO_2 was denied because of the negligibly small current density from the acetic acid fuel as mentioned before.

For the two-step with the three-pathway mechanism, the following kinetic equations were derived assuming that the rate of each electrochemical reaction was a first order of the concentration of the related compounds;

$$r_{\text{CH}_3\text{COOH}} = \frac{dM_{\text{CH}_3\text{CHO}}}{dt} = k_1 C_{\text{C}_2\text{H}_5\text{OH}} - k_2 C_{\text{C}_2\text{H}_5\text{OH}} - k_3 C_{\text{CO}_2} \quad (5)$$

$$r_{\text{CH}_3\text{COOH}} = \frac{dM_{\text{CH}_3\text{COOH}}}{dt} = k_2 C_{\text{CH}_3\text{CHO}} \quad (6)$$

$$r_{\text{CO}_2} = \frac{dM_{\text{CO}_2}}{dt} = k_3 C_{\text{CH}_3\text{CHO}} \quad (7)$$

where r_i is the production rate of component i and C_i is the concentration of component i in the bulk solution, k is the rate constant. By measuring the production rates and the concentrations in Eqs. (5)–(7), the rate constants k_1 to k_3 could be obtained.

Fig. 11 shows the calculated rate constants, k_1 , k_2 and k_3 , for each catalyst at 353 K, 0.5 M ethanol and the different cell voltages. The rate constant was calculated based on the loading of the metal catalyst. The value of k_1 was two orders of magnitude smaller than that of k_2 and k_3 . This is due to the big difference in the bulk concentration of ethanol and that of the reaction products, acetaldehyde or acetic acid. A limiting current appeared for all the catalysts at 0.05 V except for the case of Pt/C as shown in Fig. 2, therefore, the kinetic constants of the different catalysts were compared at 0.125 V and 0.2 V.

The rate constant k_1 , which corresponds to the reaction from ethanol to acetaldehyde, was increased by the addition of Ru and Rh for the Pt/C and PtRu/C catalysts, respectively, indicating that Ru and/or Rh additions activated this reaction path, irrespective of their proportions. For the rate constant k_2 , which corresponds to the reaction rate from acetaldehyde to acetic acid, a similar effect could be seen, except that the excess amount of Rh such as

PtRuRh(1:1:2)/C decreased the activity for the reaction. Although the addition of Ru and Rh increased the activity of the Pt/C catalyst, i.e., current and power densities, they decreased k_3 that corresponds to the activity for the reaction from acetaldehyde to CO₂, i.e., its selectivity to CO₂. This result was similar to that obtained for the Sn and Ru addition to Pt and PtSn, respectively, reported by Rousseau et al. [2], showing that the Sn and Ru addition increased the current density but did not improve the CO₂ selectivity. The product distributions for PtSn and PtSnRu were similar. They explained these results with the Sn and Ru additions by a bifunctional mechanism, for Sn, which preferentially adsorbs oxygen-containing species and a ligand effect, for Ru, that affects the electronic distribution around the Pt sites. Ru is also known to preferentially adsorb OH species which enhance the oxidation of CO species strongly adsorbed on Pt in the case of methanol oxidation. Rh addition to PtRu may induce a ligand effect similar to that of Ru in PtSnRu.

Fig. 12 shows the calculated rate constants k_2 and k_3 at 0.125 V for the case of the 0.3 M acetaldehyde fuel. The trends of the magnitude of k_2 and k_3 for the different catalysts were very similar to that for the case of 0.5 M ethanol.

The electro-oxidation of ethanol at the anode of DEFCs with different catalysts was investigated in this study. In the product analysis, an error caused by the crossover of ethanol, reaction products and also oxygen would not be neglected. However, a qualitative effect of Rh and Ru addition to PtRu and Pt, respectively, on the reaction scheme of the ethanol electro-oxidation could be revealed.

4. Conclusions

For the DEFC anode catalyst, Pt/C, PtRu(1:1)/C, PtRuRh(2:1:1)/C and PtRuRh(1:1:2)/C were prepared by the impregnation method and their catalytic activity was evaluated at 358 K with 0.05 M ethanol by measuring the DEFC performance with the different catalysts and the reaction products at the anode. The following conclusions were obtained.

- 1) It was confirmed that PtRuRh(2:1:1)/C showed a better DEFC performance, i.e., a higher current density in the DEFC than that of PtRu(1:1)/C and the other catalysts prepared.
- 2) Acetaldehyde, acetic acid and a small amount of CO₂ were detected as the anode products in accordance with the previous reports. The selectivity for acetaldehyde was dependent on the cell voltage between 0.05 and 0.2 V for the different catalysts prepared. The selectivity for acetic acid and CO₂ was independent of the cell voltage for the binary and ternary catalysts, while that for the Pt/C was dependent on the cell voltage.
- 3) Based on the simple reaction mechanism for the electro-oxidation of ethanol, it was revealed that the additions of Ru and Rh to Pt and PtRu, respectively, increased the reaction rates from ethanol to acetaldehyde and that from acetaldehyde to acetic acid but decreased the rate from acetaldehyde to CO₂. These additions also decreased the selectivity for CO₂.

References

- [1] Q. Wang, G.Q. Sun, L.H. Jiang, Q. Xin, S.G. Sun, Y.X. Jiang, S.P. Chen, Z. Jusys, R.J. Behm, *Physical Chemistry Chemical Physics* 9 (2007) 2686–2696.
- [2] S. Rousseau, C. Coutanceau, C. Lamy, J.-M. Leger, *Journal of Power Sources* 158 (2006) 18–24.
- [3] W.J. Zhou, W.Z. Li, S.Q. Song, Z.H. Zhou, L.H. Jiang, G.Q. Sun, Q. Xin, K. Poulianitis, S. Kontou, P. Tsiakaras, *Journal of Power Sources* 131 (2004) 217–223.
- [4] H. Wang, Z. Jusys, R.J. Behm, *Journal Power Sources* 154 (2006) 351–359.
- [5] V. Rao, C. Cremers, U. Stimming, L. Cao, S. Sun, S. Yan, G. Sun, Q. Xin, *Journal of the Electrochemical Society* 145 (2007) B1138–B1147.
- [6] E. Antolini, F. Colmati, E.R. Gonzalez, *Electrochemistry Communications* 9 (2007) 398–404.
- [7] A. Kowal, M. Li, M. Shao, K. Sasaki, M.B. Vukmirovic, J. Zhang, N.S. Marinkovic, P. Liu, A.I. Frenkel, R.R. Adzic, *Nature Materials* 8 (2009) 325–330.
- [8] N. Nakagawa, T. Watanabe, M. Wagatsuma, T. Tsujiguchi, *Key Materials Engineering*, in press.
- [9] E.V. Spinacé, M. Linardi, A.O. Neto, *Electrochemistry Communications* 7 (2005) 365–369.
- [10] E. Lee, A. Murthy, A. Manthiram, *Electrochimica Acta* 56 (2011) 1611–1618.
- [11] J. Ribeiro, D.M. dos Anjos, K.B. Kokoh, C. Coutanceau, J.M. Léger, P. Olivi, A.R. deAndrade, G. Tremiliosi-Filho, *Electrochimica Acta* 52 (2007) 6997–7006.
- [12] E.V. Spinace, R.R. Dias, M. Brandalise, M. Linardi, A.O. Neto, *Ionics* 16 (2010) 91–95.
- [13] B.R.F. De Souza, M.M. Tui, M. Brandalise, R.R. Dias, M. Linardi, E.V. Sminace, M.C. dos Santos, A.O. Neto, *International Journal of Electrochemical Science* 5 (2010) 895–902.
- [14] J.E. Thomas, A.R. Bonesi, M.S. Moreno, A. Visintin, A.M. Castro Luna, W.E. Triaca, *International Hydrogen Energy* 35 (2010) 11681–11686.
- [15] X. Zhao, W. Li, L. Jiang, W. Zhou, Q. Xin, B. Yi, G. Sun, *Carbon* 42 (2004) 3263–3265.
- [16] D.D. James, D.V. Bennett, G. Li, A. Ghumman, R.J. Helleur, P.G. Pickup, *Electrochemistry Communications* 11 (2009) 1877–1880.
- [17] J.P.I. de Souza, S.L. Queiroz, K. Bergamaski, E.R. Gonzalez, F.C. Nart, *The Journal of Physical Chemistry B* 106 (2002) 9825–9830.
- [18] S. Kontou, V. Stergiopoulos, S. Song, P. Tsiakaras, *Journal of Power Sources* 171 (2007) 1–7.
- [19] A. Jablonski, P.J. Kulesza, A. Lewera, *Journal of Power Sources* 196 (2011) 4714–4718.
- [20] D.D. James, P.G. Pickup, *Electrochimica Acta* 55 (2010) 3824–3829.
- [21] H. Wang, Z. Jusys, R.J. Behm, *The Journal of Physical Chemistry B* 108 (2004) 19413–21924.
- [22] R. Ianniello, V.M. Schmidt, J.L. Rodriguez, E. Pastor, *Journal of Electroanalytical Chemistry* 471 (1999) 167–179.